



## An example of multicomponent magnetization in welded tuffs: a case study of Upper Cretaceous welded tuffs of eastern Russia

Koji Uno<sup>a,b,\*</sup>, Yo-ichiro Otofujii<sup>c</sup>, Takaaki Matsuda<sup>d,†</sup>, Kuniyuki Furukawa<sup>b</sup>, Toshiaki Mishima<sup>a</sup>,  
Yoshiki Kuniko<sup>c</sup>, Ryo Enami<sup>c</sup>, Ruslan G. Kulinich<sup>e</sup>, Petr S. Zimin<sup>e</sup>, Anatoly P. Matunin<sup>f</sup>,  
Vladimir G. Sakhno<sup>f</sup>

<sup>a</sup>Division of Global Development Science, Graduate School of Science and Technology, Kobe University, Kobe, Japan

<sup>b</sup>Department of Environmental Sciences, Faculty of Integrated Human Studies, Kyoto University, Sakyo-ku, Kyoto 606-8501, Japan

<sup>c</sup>Department of Earth and Planetary Sciences, Faculty of Science, Kobe University, Kobe, Japan

<sup>d</sup>Department of Geology, Faculty of Science, Himeji Institute of Technology, Himeji, Japan

<sup>e</sup>Pacific Oceanological Institute, Russian Academy of Science, Vladivostok, Russian Federation

<sup>f</sup>Far East Geological Institute, Russian Academy of Science, Vladivostok, Russian Federation

Received 27 May 2001; revised 24 May 2002; accepted 24 May 2002

### Abstract

Four distinct components of natural remanent magnetization were isolated from a single site in welded tuffs in the Upper Cretaceous Kisin Group of the Sikhote Alin mountain range, Russia. In order to contribute toward a basis for an interpretation of multicomponent magnetization, rock magnetic experiments were performed on the welded tuffs. All four magnetization components essentially reside in magnetite. The lowest-temperature component up to 300 °C (component A:  $D = 349.3^\circ$ ,  $I = 60.9^\circ$ ,  $\alpha_{95} = 7.3^\circ$ ,  $N = 7$ ) is a present day viscous magnetization. The third-removed component (component C:  $D = 41.4^\circ$ ,  $I = 51.8^\circ$ ,  $\alpha_{95} = 3.5^\circ$ ,  $N = 8$ ), isolated over the temperature range of 450–560 °C, is a primary remanence. The second- and fourth-demagnetized components (component B:  $D = 174.7^\circ$ ,  $I = -53.1^\circ$ ,  $\alpha_{95} = 21.2^\circ$ ,  $N = 3$  and component D:  $D = 188.1^\circ$ ,  $I = -64.5^\circ$ ,  $\alpha_{95} = 4.0^\circ$ ,  $N = 8$ , respectively) are secondary magnetizations related to a thermal event in Sikhote Alin between 66 and 51 Ma. Components B and D were acquired through different remagnetization processes. Component B is ascribed to a thermoviscous remanent magnetization carried by single-domain magnetite, and component D is a chemical remanent magnetization.

© 2002 Elsevier Science Ltd. All rights reserved.

**Keywords:** Remanent magnetization; Cretaceous; Russia

### 1. Introduction

Multiple components of remanent magnetization are often identified in a single sample. Numerous studies have shown that a primary magnetization is generally observed at high unblocking temperatures during thermal demagnetization and often appears only after removal of secondary magnetization components. Alternatively all components of remanent magnetization may be of secondary origin (Banerjee et al., 1997). Recently,

Dunlop et al. (1997a) reported a primary magnetization removed prior to a secondary magnetization during thermal demagnetization. They suggested that chemical growth of secondary magnetite and hematite explains the higher unblocking temperatures of the secondary components than that of the primary component.

Paleomagnetic investigation of welded tuffs in the Upper Cretaceous Kisin Group of the Sikhote Alin mountain range, eastern Russia (Fig. 1(a)), has revealed two high unblocking temperature magnetizations (Uno et al., 1999). The high unblocking temperature component, of normal polarity, is a primary magnetization (unblocking temperatures of 590–680 °C). That of reversed polarity is a secondary component (unblocking temperatures of 590–620 °C), as ascertained by fold tests (McFadden, 1990) at the 95% confidence level (Fig. 1(c)). The post-folding reversed polarity magnetizations are

\* Corresponding author. Present address: Department of Environmental Sciences, Faculty of Integrated Human Studies, Kyoto University, Sakyo-ku, Kyoto 606-8501, Japan. Tel.: +81-75-753-6717; fax: +81-75-753-6872.

E-mail address: unokoji@gaia.h.kyoto-u.ac.jp (K. Uno).

† Died of myocardial infarction on September 12, 2001.

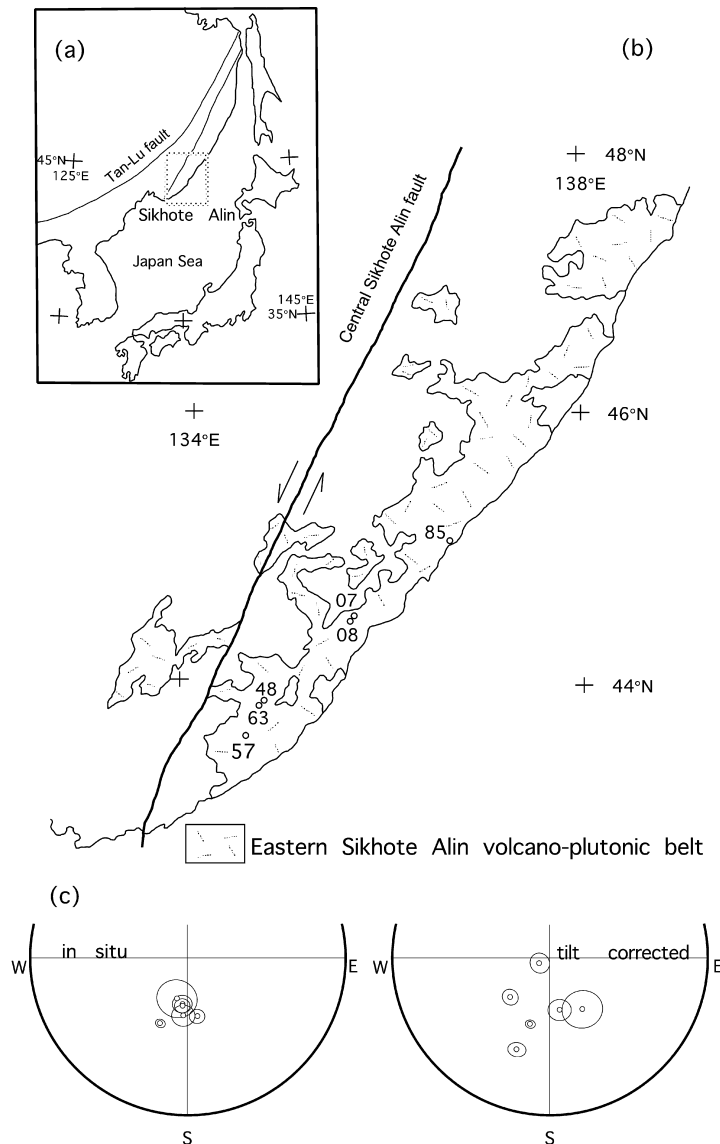


Fig. 1. (a) Sketch map of Sikhote Alin and adjacent area. (b) Geologic map of the study area. SA57 is the paleomagnetic sampling site for this study. The six sampling sites (open circles) showed the high temperature component of reversed polarity with a negative fold test (Uno et al., 1999). (c) Equal area projections of paleomagnetic directions for the six sites showing the negative fold test.

ascribed to remagnetization between 66 and 51 Ma. The reversed polarity data from six sampling sites (Fig. 1(b)), before tilt correction, are parallel to the characteristic direction of younger welded tuffs formed by the igneous activity between 66 and 51 Ma in Sikhote Alin (Otofujii et al., 1995).

Site SA57, reported by Uno et al. (1999), is one of six remagnetized sites, and exhibited the most complex demagnetization behavior of remanent magnetization (Fig. 2). Four components of remanent magnetization were resolved during thermal demagnetization. The highest-temperature component at the site was interpreted as a secondary magnetization. Uno et al. (1999) dismissed the other three components as low unblocking temperature magnetizations of little importance.

A multicomponent magnetization merits discussing because it may record the history of a study area, but such

complex behavior tends to be excluded from discussions when it occurs as a small minority. Here we reconsider the origin of the complex magnetization behavior in the Kisin welded tuffs using site SA57 as a focus of study. The availability of samples with four-component magnetization was restricted to this area and we recognize that this study is based on a small number of samples from a single site; however, our rock magnetic experiments provide a basis for an interpretation of multicomponent magnetization.

## 2. Geologic setting and sampling

The basement of the Sikhote Alin mountain range consists mainly of an Upper Jurassic accretionary complex (Samarkinsk complex) and Lower Cretaceous turbidites

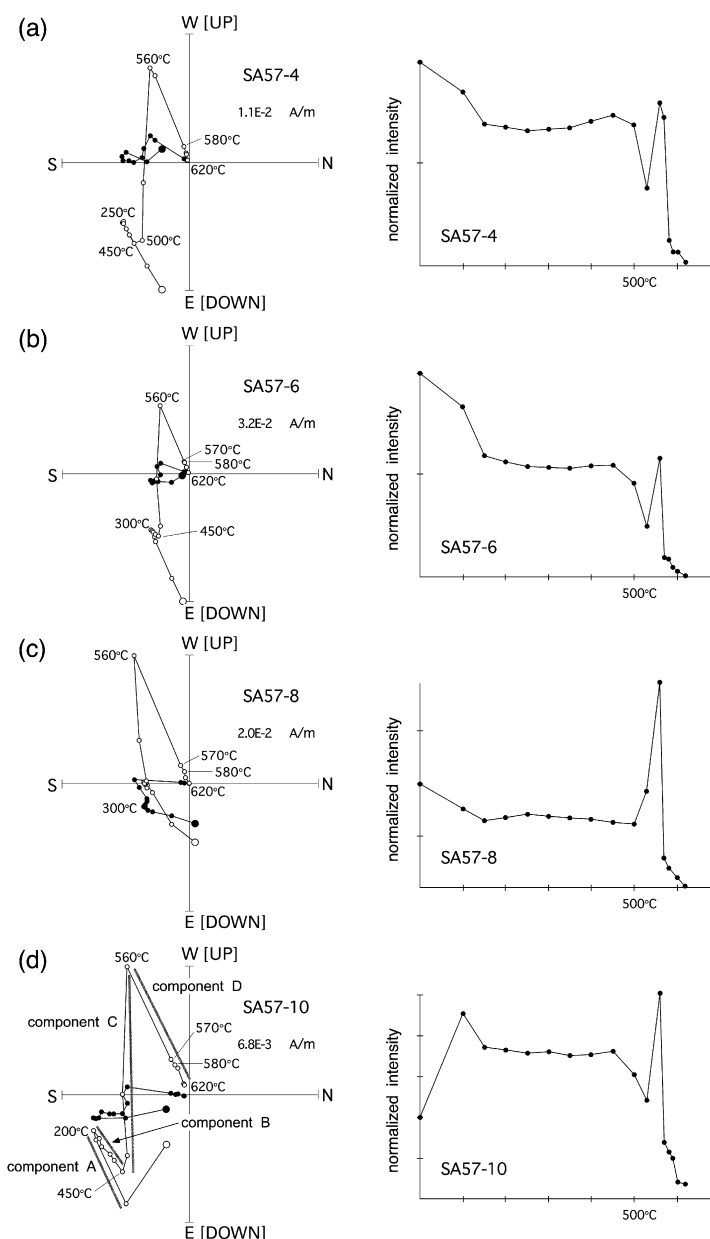


Fig. 2. Orthogonal plots of thermal demagnetization results (before tilt correction) and normalized remanence intensity curves of site SA57. Solid and open symbols in demagnetization diagrams represent projections on horizontal and vertical planes, respectively.

(Zhuravlevsk-Tummin belt) (Natal'in, 1993). Sikhote Alin is cut by a sinistral fault trending NE–SW (central Sikhote Alin fault) with a lateral offset of about 200–250 km.

Late Cretaceous to Paleogene igneous activity occurred in the eastern Sikhote Alin and produced volcanic rocks locally more than 1000 m in thickness (eastern Sikhote Alin volcano-plutonic belt) (Kirillova, 1995). The Upper Cretaceous to Paleogene volcanic rocks are divided into six volcanic groups: the Sinancha, Kisin, Sijanov, Bogopol, Tadusi, and Suvolov Groups in ascending order (Matunin, 1988). The Kisin Group is of Late Cretaceous age as indicated by *Osmunda azuwensis* Tanai, *Cladophlebis frigida* Heer and *Sequaia fastigiata* Heer (Matunin, 1988; Sakhno et al., 1991). The Sijanov and

Bogopol welded tuffs are K–Ar dated at 66.0 and 52.6–50.6 Ma, respectively (Otofuji et al., 1995).

Ten hand samples of welded tuffs in the Kisin Group were collected at site SA57 located in the southern part of Sikhote Alin (43.57°N, 134.66°E) (Fig. 1(b)), but two samples (SA57-3 and 5) were lost during transportation. The site is about 50 km from the central Sikhote Alin fault and 5 km from the distribution area of the Sijanov and Bogopol Groups and coeval granites. The eutaxitic structure at this site (strike/dip = 305°/29°) was measured as the bedding plane for tilt correction. Tilting of the Kisin Group occurred prior to the Neogene because Neogene rocks in this area are not tilted (Bretstein, 1988).

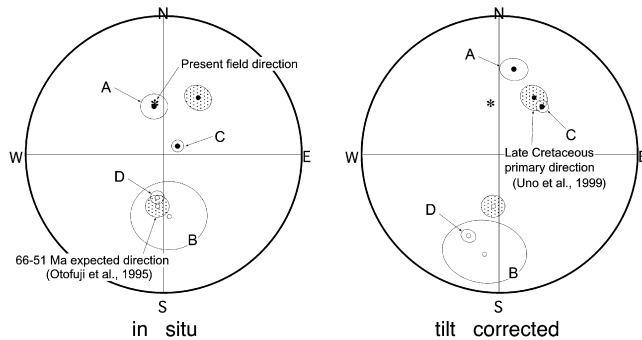


Fig. 3. Equal area projections of the four directions of magnetization identified in site SA57 (with associated 95% confidence circles) drawn with the present Earth's field direction, the 66–51 Ma expected direction of Sikhote Alin (Otofuji et al., 1995) and the Late Cretaceous primary direction of the Kisin Group (Uno et al., 1999).

### 3. Paleomagnetic and rock magnetic methods

In the laboratory, individual specimens 25 mm in diameter and 22 mm long were prepared from each hand sample. Natural remanent magnetizations (NRMs) were measured with a 2-G cryogenic magnetometer. Specimens were subjected to stepwise thermal demagnetization with a Natsuhara thermal demagnetizer in steps of 50 °C up to 500 °C, and 10 or 30 °C above 500 °C. Results for each specimen were analyzed using orthogonal vector diagrams and principal component analysis (Zijderveld, 1967; Kirschvink, 1980).

We performed stepwise acquisition of isothermal remanent magnetization (IRM) up to the maximum field of 2.7 T along the Z-axis of specimens with a 2-G pulse magnetizer. Thermal demagnetization of the orthogonal three-component IRM (Lowrie, 1990) was performed with a 2-G pulse magnetizer. Specimens for the IRM measurements were previously demagnetized in a peak alternating field of 100 mT. Thermomagnetic analysis in a magnetic field of 0.8 T was carried out with a laboratory-made Curie balance. Samples were heated up to 700 °C at a constant rate of 8 °C/min and cooled at the same rate in air. Hysteresis measurement was performed using a Princeton Measurements alternating gradient force magnetometer, with a correction for high field paramagnetic slope. The low temperature behavior of SIRM with an applied field of 1.0 T at 5 K was observed with a Quantum Design magnetic property measurement system. Anisotropy of magnetic susceptibility (AMS) was measured with a Kappabridge susceptibility meter to compare directions between remanence and the maximum axis of magnetic susceptibility.

### 4. Paleomagnetism

Four distinct remanent magnetization components were isolated in individual specimens during thermal demagne-

tization (Figs. 2 and 3). The first-, second-, third- and fourth-removed components are here referred to as components A, B, C, and D, respectively (Fig. 2(d)). For each component, a mean direction is calculated (Table 1). Selected duplicate specimens from hand samples were thermally demagnetized to confirm the reliability of remanence directions and gave the same directions as those obtained from another ones (angular separation within 5°).

Component A is unblocked below 300 °C. The direction of this component before tilt correction is parallel to the present direction of the Earth's magnetic field ( $D = 349.9^\circ$ ,  $I = 59.3^\circ$ ). This component is not resolved in sample SA57-1 because of ill-defined demagnetization behavior. The mean direction of seven samples is  $D = 349.3^\circ$ ,  $I = 60.9^\circ$  before tilt correction, and  $D = 9.7^\circ$ ,  $I = 37.1^\circ$  after tilt correction ( $\alpha_{95} = 7.3^\circ$ ).

Component B is of reversed polarity. This component, relative to other components, is of low intensity and observable in three samples out of eight. The declination of this component is southward and the inclination is moderately upward before tilt correction. The maximum unblocking temperature of this component is 450 °C. The mean direction of three samples is  $D = 174.7^\circ$ ,  $I = -53.1^\circ$  before tilt correction, and  $D = 188.7^\circ$ ,  $I = -28.5^\circ$  after tilt correction ( $\alpha_{95} = 21.2^\circ$ ).

Component C is of normal polarity. This component is of relatively high intensity. Its direction is of steep inclination before tilt correction, and of northeast declination and intermediate positive inclination after tilt correction. This component is unblocked at temperature of up to 560 °C. The mean direction of eight samples is  $D = 57.7^\circ$ ,  $I = 80.2^\circ$  before tilt correction, and  $D = 41.4^\circ$ ,  $I = 51.8^\circ$  after tilt correction ( $\alpha_{95} = 3.5^\circ$ ).

Component D has a southerly declination and intermediate negative inclination. Its direction is statistically indistinguishable from that of component B. A large decay of the component is observed between 560 and 580 °C. The component decays to the origin of the orthogonal vector diagram. The mean direction of eight samples is  $D = 188.1^\circ$ ,  $I = -64.5^\circ$  before tilt correction, and  $D = 201.1^\circ$ ,  $I = -37.2^\circ$  after tilt correction ( $\alpha_{95} = 4.0^\circ$ ).

Observations of orthogonal vector diagrams reveal that components B and D are not the same component, but two discrete magnetization components. Component C is isolated between about 300–450 and 560 °C and lies between the unblocking temperature ranges of components B and D. The sharp demarcation in the orthogonal vector diagram between normal component C and reversed components D and B suggests that little overlap of the unblocking temperature spectra exists between these components (Fig. 2(d)). Components B and D are, therefore, not a single magnetization whose unblocking range entirely encloses that of component C, although the directions of components B and D are statistically indistinguishable.

Table 1  
Paleomagnetic results of site SA57 of the Kisin Group

Sample	Component ( <i>N</i> )	Temperature range (°C)	In situ (°)		Tilt corrected (°)		<i>k</i>	$\alpha_{95}$ (°)
			<i>D</i>	<i>I</i>	<i>D</i>	<i>I</i>		
SK57-2	A	NRM-300	340.5	48.7	359.4	28.7		
SK57-4	A	NRM-250	343.5	60.6	5.8	37.9		
SK57-6	A	NRM-300	340.3	66.7	8.4	43.8		
SK57-7	A	100–250	344.6	58.1	6.3	36.6		
SK57-8	A	NRM-300	6.7	51.0	15.9	24.3		
SK57-9	A	NRM-300	1.6	72.1	21.1	45.1		
SK57-10	A	100–200	349.4	66.4	12.5	41.7		
Mean	7		349.3	60.9	9.7	37.1	70.1	7.3
SK57-4	B	250–450	178.1	–63.7	195.2	–37.9		
SK57-6	B	350–450	182.5	–40.1	190.1	–14.4		
SK57-10	B	200–450	161.7	–54.4	181.1	–32.8		
Mean	3		174.7	–53.1	188.7	–28.5	34.7	21.2
SK57-1	C	450–560	40.9	77.5	36.9	48.5		
SK57-2	C	450–560	49.8	75.5	40.3	46.8		
SK57-4	C	500–560	101.7	82.5	47.7	57.4		
SK57-6	C	450–560	86.5	82.2	45.8	55.7		
SK57-7	C	350–560	46.0	76.7	41.3	47.8		
SK57-8	C	300–560	54.8	77.3	41.4	48.8		
SK57-9	C	400–560	44.6	79.9	37.5	51.1		
SK57-10	C	500–560	86.7	85.5	41.7	58.0		
Mean	8		57.7	80.2	41.4	51.8	253.9	3.5
SK57-1	D	560–590	193.8	–65.1	203.9	–37.1		
SK57-2	D	560–620	181.8	–67.3	198.9	–40.6		
SK57-4	D	560–620	204.9	–64.9	209.7	–36.1		
SK57-6	D	560–620	189.5	–66.1	202.1	–38.5		
SK57-7	D	560–590	198.2	–60.3	206.9	–32.3		
SK57-8	D	560–620	175.0	–67.5	195.7	–41.7		
SK57-9	D	560–620	183.6	–57.6	195.9	–31.1		
SK57-10	D	560–620	175.9	–64.8	194.7	–39.1		
Mean	8		188.1	–64.5	201.1	–37.2	192.1	4.0

Component: components A–D are according to the order of their appearance; *N*, the number of the samples in calculation for the means; *D* and *I*, declination and inclination, respectively; *k*, the precision parameter;  $\alpha_{95}$ , radius of the cone of the 95% confidence.

## 5. Rock magnetism

IRM acquisition data reveal a low coercive force with a sharp rise up to 0.2 T (Fig. 4(a)), where more than 90% of the maximum IRM has been acquired. Thermal demagnetization of the orthogonal three-component IRM reveals that the low-coercivity (<120 mT) magnetization is dominant and is unblocked at temperatures around 580 °C (Fig. 4(b)), indicating magnetite as a predominant carrier of remanent magnetization. Thermomagnetic results show a dominant Curie temperature of about 580 °C in heating (Fig. 4(c)). The Curie temperature is diagnostic of magnetite. The heating and cooling curves are similar in shape. The results of these experiments suggest that all the magnetization components essentially reside in magnetite. Although maghemite from oxidation of magnetite appears to contribute to component D in remanent magnetization, it is not observed from the rock magnetic results.

The hysteresis loop closes at an applied field of about 300 mT (Fig. 4(d)). This also suggests a low-coercivity magnetic mineral. The values of  $M_{rs}/M_s$  (remanence ratios) range from 0.11 to 0.30, while those of  $H_{cr}/H_c$  (coercivity ratios) range from 2.1 to 4.6. The values of  $H_{cr}$  (remanent coercivities) ranging between 37 and 113 mT, with a mean of 78 mT, suggest that the remanence carrying mineral is mainly in a smaller domain state, probably in a single-domain state.

Low temperature measurements of SIRM exhibit the Verwey transition at 120 K (Fig. 4(e)) and an unresolved fluctuation around 100 K. This Verwey transition is indicative of multidomain magnetite (Roberts et al., 1995) and/or stoichiometric magnetite (Özdemir et al., 1993). Because Roberts et al. (1995) suggested that stoichiometric magnetite is generally uncommon in natural rock samples, the signal at 120 K is interpreted as due to the probable presence of multidomain magnetite.

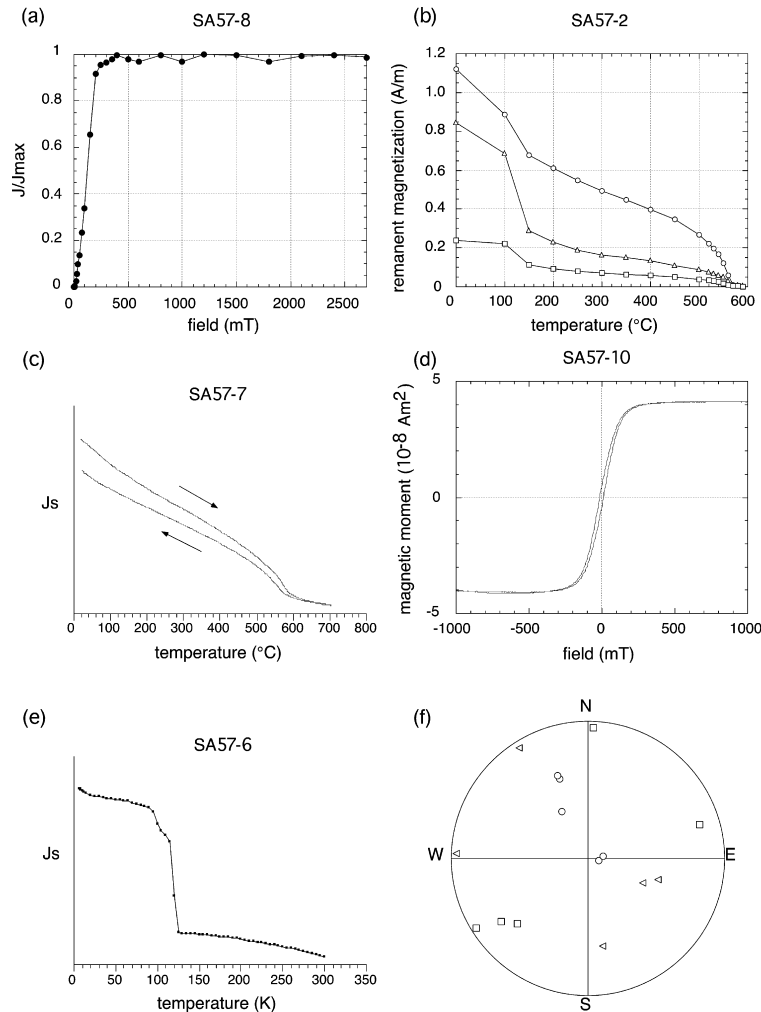


Fig. 4. Rock magnetic results. (a) Stepwise IRM acquisition. (b) Thermal demagnetization of the orthogonal three-component IRM: circles indicate soft component, 0.12 T field; triangles indicate medium component, 0.4 T field; squares indicate hard component, 2.7 T field. (c) Thermomagnetic analysis in air. (d) Hysteresis loop. (e) Low temperature measurement of SIRM. (f) Equal area projection of directions of the maximum (squares), intermediate (triangles) and minimum (circles) axes of the ARM ellipsoids (after tilt correction). All directions are plotted on the upper hemisphere.

## 6. Discussion

### 6.1. Determination of magnetization ages from comparison of Sikhote Alin paleomagnetic directions

The ages of acquisition of the four magnetization components are assigned by comparison of their directions with the present Earth's field direction, 66–51 Ma expected directions, and paleomagnetic directions of the Kisin Group in Sikhote Alin.

Component A was probably acquired in the Brunhes chron because the direction of this magnetization before tilt correction (Fig. 3) is parallel to the present Earth's field direction ( $D = 349.9^\circ$ ,  $I = 59.3^\circ$ ).

The direction of the reversed polarity component B, before tilt correction, is statistically indistinguishable from the averaged field direction in Sikhote Alin during the time period of 66–51 Ma ( $D = 187.0^\circ$ ,  $I = -58.7^\circ$  with  $\alpha_{95} = 6.5^\circ$ ) as calculated from the 66 Ma Sijanov Group and the

51 Ma Bogopol Group (Otofuji et al., 1995). Component B is considered to be a secondary magnetization acquired between 66 and 51 Ma.

Component C is interpreted to be a primary paleomagnetic record for the Kisin Group. The direction of component C after tilt correction is parallel to the characteristic primary direction of the Kisin Group ( $D = 31.1^\circ$ ,  $I = 50.5^\circ$  with  $\alpha_{95} = 7.6^\circ$ ) (site SA83 in Uno et al., 1999). The direction of component C, together with previously reported primary ones, yields a positive fold test (McFadden, 1990) at the 95% confidence level. The positive inclination of component C suggests that this component is not secondary, because secondary magnetizations in the Kisin Group are uniformly of reversed polarity (Uno et al., 1999). Component C is interpreted to be of Late Cretaceous age.

Component D, of reversed polarity, is probably a secondary magnetization acquired between 66 and 51 Ma. The direction of component D, before tilt correction, is

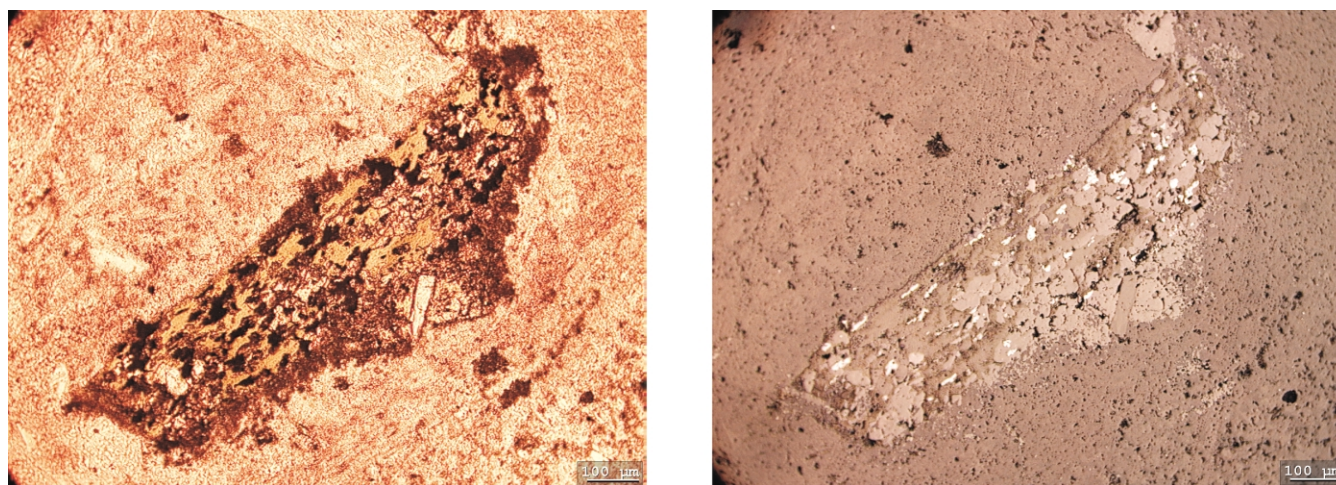


Fig. 5. Photomicrographs of sample SA57-6 showing chlorite with magnetic inclusions. Transmitted light (left) and reflected light (right).

parallel to the paleomagnetic direction representative of Sikhote Alin between 66 and 51 Ma (Otofujii et al., 1995). The post-folding nature of component D is shown by the negative fold test involving the highest unblocking temperature components from the six sites of the Kisin Group (Fig. 1(b) and (c)) (Uno et al., 1999).

The directions of the observed remanent magnetizations are not controlled by a magnetic fabric in the welded tuffs, as ascertained by AMS results. The directions of each principal axis in the AMS ellipsoid are scattered (Fig. 4(f)). A large uncertainty in the mean AMS principal axes is observed: tilt corrected directions of  $k_{\max}$  and  $k_{\min}$  are  $D = 225.1^\circ$ ,  $I = -16.4^\circ$  with  $\alpha_{95} = 25.2^\circ$  and  $D = 342.9^\circ$ ,  $I = -55.0^\circ$  with  $\alpha_{95} = 26.1^\circ$ , respectively. Both the lineation ( $k_{\max}/k_{\text{int}}$ ) and foliation ( $k_{\text{int}}/k_{\min}$ ) of magnetic susceptibility are less than 1.015 and not significant. There is no correlation between directions of the AMS maximum axes and remanence directions. The remanent magnetization components are therefore concluded to be a high-fidelity record of geomagnetic field directions in Sikhote Alin.

## 6.2. Origin of the secondary remanent magnetizations

Components A, B, and D are interpreted as secondary magnetization components, while component C is a primary magnetization, probably of thermoremanent magnetization originating from the time of formation of the welded tuffs.

Component A is a present day viscous overprint. Unblocking temperatures up to 300 °C are explained by the relaxation time-blocking temperature relations of Middleton and Schmidt (1982), assuming a mixture of single-domain and multidomain magnetite grains. Exposure to the Earth's field during the last 0.8 Ma results in laboratory unblocking temperatures of about 300 °C.

Component B is a thermoviscous remanent magnetization component carried by single-domain magnetite, with an

unblocking temperature of 450 °C. Thermal remagnetization in the Sikhote Alin area occurred between about 66 and 51 Ma and the temperature of the thermal event rose to 350–400 °C (Faure et al., 1995). The temperature of the thermal event is estimated from closure temperatures of biotite and muscovite in  $^{40}\text{Ar}/^{39}\text{Ar}$  dating. Because the duration of reversed polarity chrons during the time period of 66–51 Ma are a few million years (Cande and Kent, 1995), the unblocking temperature of 450 °C for component B gives an expected remagnetization temperature of about 360 °C, based on the relaxation time-blocking temperature relations for single-domain magnetite (Pullaiah et al., 1975). This inferred remagnetization temperature of 360 °C for component B is consistent with the independent temperature estimates of Sikhote Alin during the 66–51 Ma time period (Faure et al., 1995).

If we assume that component B was carried by multi-domain magnetite as well as single-domain magnetite, the relaxation time-blocking temperature relations of Middleton and Schmidt (1982) would predict an expected remagnetization temperature of about 550 °C. Because Faure et al. (1995) claimed that the peak temperature of the thermal event did not exceed 500 °C, we suspect that the contribution of multidomain magnetite to component B can be ruled out.

Component D is best interpreted as a chemical remanent magnetization (CRM). A large fraction of component D is demagnetized between 560 and 580 °C (Fig. 2). This component has a 'thermally discrete' unblocking temperature range, which suggests a CRM as proposed by Dunlop et al. (1997b).

The higher unblocking temperature for component D than that of the primary component C also implies a chemical overprint rather than a thermoviscous overprint, because a chemical overprint can have a higher unblocking temperature range than that of a primary thermoremanence. Dunlop et al. (1997a) observed a hydrothermal chemical overprint with higher unblocking temperatures (550–600 °C) than those of

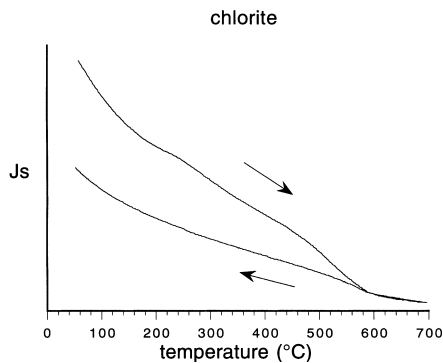


Fig. 6. Thermomagnetic analysis of separated chlorite fractions from crushed samples of site SA57 (in air).

the primary component (300–550 °C) carried mainly by magnetite. The example is similar to that of the present study.

The large decay in intensity between 560 and 580 °C suggests that magnetite is the predominant carrier of the chemical remanence; however, the remanence is eventually unblocked at 620 °C for six samples out of eight (Table 1). Because the IRM acquisition and hysteresis results show no or little contribution from a high-coercivity mineral (i.e. hematite is not significant), the unblocking temperature of 620 °C is interpreted to be due to the presence of maghemite.

We observed the welded tuffs under an optical microscope, and alteration was observed. Examinations of polished sections under the transmitted light indicate that biotite has been completely replaced by chlorite (Fig. 5). One of the main alteration effects, under the reflected light, is the production of abundant opaque inclusions in the chlorite. These aspects of alteration are observed in all the samples. Thermomagnetic analysis of separated chlorite fractions from crushed samples shows that these magnetic inclusions are mainly magnetite and contain minor amounts of maghemite, the presence of which is suggested from the inflection of the heating curve and the reduction of the induced magnetization after heating (Fig. 6). It is therefore considered that the magnetic minerals in the chlorite are secondarily formed during the alteration of biotite to chlorite and are responsible for the chemical remanence.

## 7. Conclusions

We conclude that the four distinct remanent magnetization components of the welded tuffs in the Kisin Group are essentially carried by magnetite. The welded tuffs preserve a primary component (C), which is unblocked at a temperature range between those of secondary components B and D. Component B is ascribed to a thermoviscous remanence carried by single-domain magnetite, and component D is a hydrothermal chemical remanence. Thermal perturbation in Sikhote Alin between 66 and 51 Ma was the cause of remagnetization.

## Acknowledgments

The logistics in this work were set up by the Pacific Oceanological Institute (POI), Russia. We express our gratitude to Dr V.M. Nikiforov, Dr Y. Pochkay and Dr M.V. Radchenko for helpful cooperation in the field. Dr G.M. Turner provided thoughtful reviews to improve the quality of this paper. We are grateful to Dr E. McClelland and Dr M. Bazhenov for valuable suggestions for improving the manuscript. This work has benefited from extensive discussions with Dr N. Ishikawa. We thank Dr M. Torii for his kind help to perform low temperature experiments. This work was supported in part by the Grants-in-aid (Nos. 08041110, 09440175) from the Japanese Ministry of Education, Science and Culture.

## References

- Banerjee, S., Elmore, R.D., Engel, M.H., 1997. Chemical remagnetization and diagenesis: testing the hypothesis in the Pennsylvanian Belden Formation, Colorado. *Journal of Geophysical Research* 102, 24825–24842.
- Bretstein, Yu.S., 1988. Magnetic properties of Late Cretaceous–Cenozoic volcanic rocks of the Soviet Far East South. *Journal of Physics of the Earth* 36, 39–64.
- Cande, S.C., Kent, D.V., 1995. Revised calibration of the geomagnetic polarity timescale for the Late Cretaceous and Cenozoic. *Journal of Geophysical Research* 100, 6093–6095.
- Dunlop, D.J., Schmidt, P.W., Özdemir, Ö., Clark, D.A., 1997a. Paleomagnetic and paleothermometry of the Sydney Basin 1. Thermoviscous and chemical overprinting of the Milton Monzonite. *Journal of Geophysical Research* 102, 27271–27283.
- Dunlop, D.J., Özdemir, Ö., Schmidt, P.W., 1997b. Paleomagnetic and paleothermometry of the Sydney Basin 2. Origin of anomalously high unblocking temperatures. *Journal of Geophysical Research* 102, 27285–27295.
- Faure, M., Natal'in, B.A., Monié, P., Vrublevsky, A.A., Borukaiev, Ch., Prikhodko, V., 1995. Tectonic evolution of the Anuy metamorphic rocks (Sikhote Alin, Russia) and their place in the Mesozoic geodynamic framework of East Asia. *Tectonophysics* 241, 279–301.
- Kirillova, G.L., 1995. Late Mesozoic environmental history of southeastern Russia. In: Chang, K.H., Park, S.O. (Eds.), *Environmental and Tectonic History of East and South Asia*, Kyungpook National University, Taegu, Korea, pp. 93–107.
- Kirschvink, J.L., 1980. The least-squares line and plane and analysis of palaeomagnetic data. *Geophysical Journal of the Royal Astronomical Society* 62, 699–718.
- Lowrie, W., 1990. Identification of ferromagnetic minerals in a rock by coercivity and unblocking temperature properties. *Geophysical Research Letters* 17, 159–162.
- Matunin, A.P., 1988. Magmatism evolution of Kavaleroovskaya ore-magmatic system. In: Sheglov, A.D., Zimin, S.S. (Eds.), *Magmatism of Ore Areas and Kongs (Primorye)*, USSR Academy of Sciences, Far-Eastern Branch, Vladivostok, pp. 83–88.
- McFadden, P.L., 1990. A new fold test for palaeomagnetic studies. *Geophysical Journal International* 103, 163–169.
- Middleton, M.F., Schmidt, P.W., 1982. Paleothermometry of the Sydney Basin. *Journal of Geophysical Research* 87, 5351–5359.
- Natal'in, B.A., 1993. History and modes of Mesozoic accretion in Southeastern Russia. *Island, Arc* 2, 15–34.
- Otofuji, Y., Matsuda, T., Itaya, T., Shibata, T., Matsumoto, M., Yamamoto, T., Morimoto, C., Kulinich, R.G., Zimin, P.S., Matunin, A.P., Sakhno,



- V.G., Kimura, K., 1995. Late Cretaceous to early Paleogene paleomagnetic results from Sikhote Alin, far eastern Russia: implications for deformation of East Asia. *Earth and Planetary Science Letters* 130, 95–108.
- Özdemir, Ö., Dunlop, D.J., Moskowitz, B.M., 1993. The effect of oxidation on the Verway transition in magnetite. *Geophysical Research Letters* 21, 757–760.
- Pullaiah, G., Irving, E., Buchan, K.L., Dunlop, D.J., 1975. Magnetization changes caused by burial and uplift. *Earth and Planetary Science Letters* 28, 133–143.
- Roberts, A.P., Cui, Y., Verosub, K.L., 1995. Wasp-waisted hysteresis loops: mineral magnetic characteristics and discrimination of components in mixed magnetic systems. *Journal of Geophysical Research* 100, 17909–17924.
- Sakhno, V.G., Matunin, A.P., Martynov, Yu.A., Popov, V.K., Polin, V.F., 1991. East-Sikhote-Alinsky volcanic belts. In: Sheglov, A.D., Zimin, S.S. (Eds.), *Magmatism of Asian Eastern Margin*, Nauka, Moscow, pp. 99–110.
- Uno, K., Otofujii, Y., Matsuda, T., Kuniko, Y., Enami, R., Kulinich, R.G., Zimin, P.S., Matunin, A.P., Sakhno, V.G., 1999. Late Cretaceous paleomagnetic results from Northeast Asian continental margin: the Sikhote Alin mountain range, eastern Russia. *Geophysical Research Letters* 26, 553–556.
- Zijderveld, J.D.A., 1967. A.C. demagnetization of rocks: analysis of results. In: Collinson, D.W., Creer, K.M., Runcorn, S.K. (Eds.), *Methods in Paleomagnetism*, Elsevier, Amsterdam, pp. 254–286.